Bioorganic & Medicinal Chemistry 22 (2014) 787–795

Contents lists available at ScienceDirect

Bioorganic & Medicinal Chemistry

journal homepage: www.elsevier.com/locate/bmc

Structural studies, homology modeling and molecular docking of novel non-competitive antagonists of GluK1/GluK2 receptors

Agnieszka A. Kaczor [a,b,*], Zbigniew Karczmarzyk [c], Andrzej Fruziński [d], Kalevi Pihlaja [e], Jari Sinkkonen [e], Kirsti Wiinämaki [e], Christiane Kronbach [f], Klaus Unverferth [f], Antti Poso [b], Dariusz Matosiuk [a]

[a] Department of Synthesis and Chemical Technology of Pharmaceutical Substances with Computer Modeling Lab, Faculty of Pharmacy with Division of Medical Analytics, 4A Chodźki St., PL-20093 Lublin, Poland
[b] School of Pharmacy, University of Eastern Finland, Yliopistonranta 1, PO Box 1627, FI-70211 Kuopio, Finland
[c] Department of Chemistry, Siedlce University, 3 Maja 54 St., PL-08110 Siedlce, Poland
[d] Institute of General and Ecological Chemistry, Technical University, Żeromskiego115 St.,PL-90924 Łódź, Poland
[e] Department of Chemistry, University of Turku, Vatselankatu 2, FI-20014 Turku, Finland
[f] Biotie Therapie GmbH, Meissner Str. 191, DE-01445 Radebul, Germany

ARTICLE INFO

Article history:
Received 25 September 2013
Revised 2 December 2013
Accepted 5 December 2013
Available online 12 December 2013

Keywords:
Homology modeling
Indole derivatives
Kainate receptors
Molecular docking
X-ray structure determination

ABSTRACT

Non-competitive ligands of kainate receptors have focused significant attention as medicinal compounds because they seem to be better tolerated than competitive antagonists and uncompetitive blocker of these receptors. Here we present structural studies (X-ray structure determination, NMR and MS spectra) of novel indole-derived non-competitive antagonists of GluK1/GluK2 receptors, homology models of GluK1 and GluK2 receptors based on novel AMPA receptor template as well as molecular docking of ligands to their molecular targets. We find that the allosteric site is in the receptor transduction domain, in one receptor subunit, not between the two subunits as it was indicated by our earlier studies.

1. Introduction

The glutamatergic system remains an attractive molecular target for pharmacological intervention.[1–3] Ligands acting on ionotropic glutamate receptors (iGluRs: NMDA, *N*-methyl-D-aspartate; AMPA, α-amino-3-hydroxy-5-methyl-4-isooxazolepropionic acid and kainate receptors) or metabotropic glutamate receptors (mGluRs) are potential drug candidates for the treatment of neurodegenerative diseases (Alzheimer's disease, Parkinson's disease, Huntington's disease), epilepsy as well as schizophrenia, anxiety and memory disorders.[2,3] Although only a few glutamate receptors ligands turned out to clinically useful (firstly, because of a crucial role of glutamatergic system in many physiological processes and secondly—due to the unfavorable psychotropic side effects, traditionally linked with high-affinity NMDA receptor antagonists), ligands of kainate receptor subfamily seem to be especially promising.[4,5] Kainate receptors are involved in epileptogenesis and inducing synaptic plasticity, mainly via mossy fiber long-term potentiation mechanism. Thus, antagonists of kainate receptors are potential anti-seizure and neuroprotective agents. Moreover, as non-competitive antagonists of AMPA receptors are well tolerated in preclinical and clinical studies,[6] it may be expected that it will also concern such ligands of kainate receptors.

The research on non-competitive antagonists of kainate receptors is hindered by the fact that only three series of such compounds have been obtained up to now,[7–9] (Fig. 1). Recently we have reported 2,3,5-trisubstituted indoles **1**–**4** (intermediates) and 1,2,3,5-tetrasubstituted indole derivatives **5**–**10** which belong to most active non-competitive antagonists of GluK1 receptor and are the first known such ligands of GluK2 receptor (Fig. 2).[9] We also proposed a pharmacophore model for these ligands.[9] Moreover, we have suggested a binding site for them in the receptor transduction domain[10] thanks to construction of whole receptor models.[10,11] In order to build models of GluK1 and GluK2 receptors we used separate templates for each domain (transmembrane domain, transduction domain, ligand-binding domain and N-terminal domain). Although the constructed models differed significantly from the later obtained crystal structure of GluA2 receptor,[12] they exhibited the correct twofold symmetry and correct dimensions. Here we present structural studies of these

* Corresponding author. Tel.: +48 815357365; fax: +48 815357355.
E-mail addresses: agnieszka.kaczor@umlub.pl (A.A. Kaczor), darek.matosiuk@umlub.pl (D. Matosiuk).

0968-0896/$ - see front matter © 2013 Elsevier Ltd. All rights reserved.
http://dx.doi.org/10.1016/j.bmc.2013.12.013

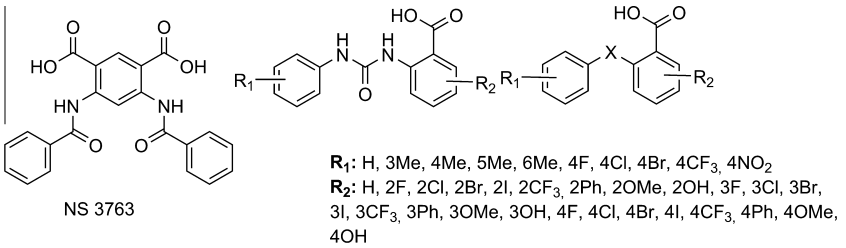

Figure 1. Non-competitive antagonists of GluK1 receptors.

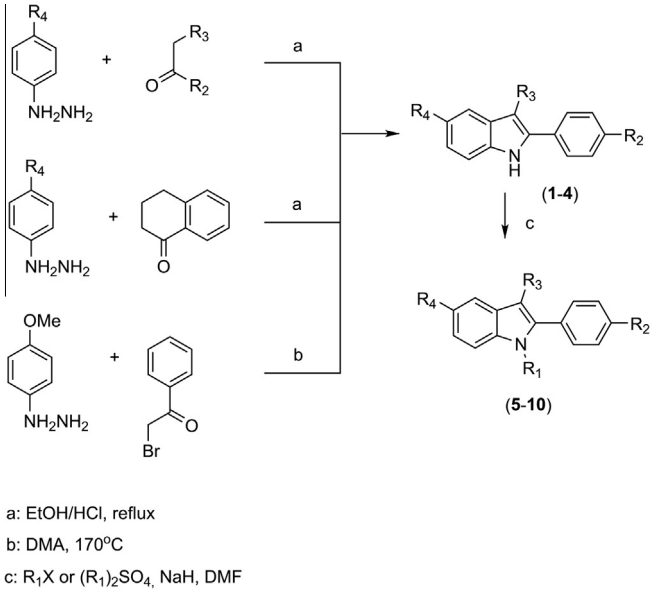

Figure 2. Synthesis of indole derivatives.

Table 1
Pharmacological activity of novel non-competitive antagonists of GluK1/GluK2 receptors, nd–not determined[8]

	R^1	R^2	R^3	R^4	IC_{50}, μM	
					GluK1	GluK2
1	H	Ph	H	OCH_3	nd	nd
2	H	4-OMePh	CH_3	H	nd	nd
3	H	Ph	CH_3	OCH_3	nd	nd
4	H	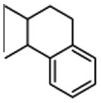		OCH_3	nd	nd
5	C_2H_5	4-OMePh	CH_3	OCH_3	4.0	0.7
6	4-ClBn	4-OMePh	CH_3	OCH_3	0% (100 μM)	20% (100 μM)
7	C_2H_5	Ph	H	OCH_3	12.0	6.7
8	C_2H_5	4-OMePh	CH_3	H	32% (100 μM)	10.0
9	C_2H_5	Ph	CH_3	OCH_3	32% (100 μM)	6.0
10	C_2H_5	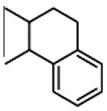		OCH_3	0% (100 μM)	1% (100 μM)

compounds, homology models of GluK1 and GluK2 receptors built using a novel AMPA GluA2 receptor template[12] and molecular docking to the transduction domain of the receptors.

2. Materials and methods

2.1. Chemistry

The intermediates 1–4 were synthesized by Fischer or Bischler indolization method and were alkylated with ethyl bromide or 4-chlorobenzyl chloride in the presence of sodium hydride in anhydrous DMF to give final compounds 5–10 as reported previously (Fig. 2).[9]

2.2. Pharmacology

The final products, **5**–**10** were tested for their affinity to GluK1 and GluK2 receptors as reported previously.[9] In particular, the investigations with the ^{3}H-kainate binding assay showed no inhibition, which makes it possible to conclude about the non-competitive type of antagonism for compounds **5**–**10**. Pharmacological data are presented in Table 1.

2.3. X-ray structure analysis

Prismatic colorless crystals of **5** and **6** suitable for X-ray diffraction analysis were grown by slow evaporation of an ethanol solution. X-ray data were collected on the Bruker SMART APEX CCD diffractometer; crystal sizes: 0.25 × 0.22 × 0.05 of **5** and 0.20 × 0.17 × 0.2 of **6**, ω scans. The multi-scan absorption correction was applied (SADABS[13]). The structures were solved by direct methods using SIR92[14] and refined by full-matrix least-squares with SHELXL97.[15] All hydrogen atoms in **5** were located in a difference Fourier map and their coordinates were refined isotropically [C–H = 0.94(3)–1.11(4) Å and U_{iso}(H) = 1.5U_{eq}(C)]. In the case of **7** the H atoms were treated as riding on their parent C atoms with C–H distances of 0.93 (aromatic), 0.97 (CH_2) and 0.96 (CH_3) and U_{iso}(H) = 1.5U_{eq}(C). The assumed absolute crystal structure of **5** was confirmed by refinement of the Flack parameter.[16] The crystal and experimental data are listed in Table 2. Molecular graphics were prepared using ORTEP3 for Windows.[17] PARST[18] and PLATON[19] were used for geometrical calculations. All calculations were performed using WINGX v. 1.64.05 package.[20] CCDC-930477 for **5** and CCDC-930478 for **6** contain the supplementary crystallographic data for this paper. These data can be obtained free of charge at http://www.ccdc.cam.ac.uk/conts/retrieving.html [or from the Cambridge Crystallographic Data Centre (CCDC), 12 Union Road, Cambridge CB2 1EZ, UK; fax: +44(0) 1223 336 033; email: deposit@ccdc.cam.ac.uk].

2.4. NMR studies

NMR spectra were acquired using Bruker Avance 500 spectrometer (equipped with BBO-5 mm-Zgrad probe) operating at 500.13 MHz for ^{1}H and 125.77 MHz for ^{13}C, respectively. Spectra were recorded at 25 °C using $CDCl_3$ as a solvent with a non-spinning sample in 5 mm NMR-tubes. Spectra were processed by a PC with Windows XP operating system and XWin-NMR software. Proton and carbon spectra were referenced internally to TMS signal using value 0.00 ppm.

Table 2
Crystal data and structure refinement for **5**and **6**

	5	**6**
Empirical formula	$C_{19}H_{21}NO_2$	$C_{24}H_{22}NO_2Cl$
Formula weight	295.37	391.88
Temperature (K)	293(2)	293(2)
Crystal system	Orthorhombic	Triclinic
Space group	$P2_12_12_1$	$P\bar{1}$
Unit cell parameters		
a (Å)	8.720(2)	9.088(2)
b (Å)	9.553(2)	12.477(3)
c (Å)	20.024(4)	18.704(4)
α (°)		87.93(3)
β (°)		87.82(3)
γ (°)		80.37(3)
V (Å^3)	1668.2(6)	2088.5(7)
Z	4	4
D_{calc} (g cm^{-3})	1.176	1.246
$F(000)$	632	824
λ (Cu Kα) (Å)	1.54178	1.54178
Cell parameters from	870 reflections	104 reflections
θ range for lattice parameters (°)	38.35–68.90	2.36–70.14
Absorption coefficient μ (mm^{-1})	0.600	1.761
T_{min}/T_{max}	0.864/0.971	0.720/0.966
θ Range for data collection (°)	4.42–70.05	9.30–39.80
Index ranges h, k, l	−10/10, −11/11, −24/24	−11/11, −15/15, −22/22
No. of measured reflections	19196	24160
No. of independent reflections	3166(R_{int} = 0.0192)	7612 (R_{int} = 0.0187)
No. of observed reflections	3054 with $I > 2\sigma(I)$	6148 with $I > 2\sigma(I)$
Refinement method	Full-matrix least-squares on F^2	Full-matrix least-squares on F^2
Final R indices: R, $wR(F^2)$	0.0337, 0.1019	0.0502, 0.1476
Goodness-of-fit on F^2, S	1.034	1.137
Data/parameters	3166/264	7612/506
Extinction coefficient	0.0070(7)	0.0011(3)
Flack parameter	0.1(2)	0.1(2)
	+0.134 and −0.131	+0.309 and −0.364
Largest diff. peak and hole (e Å^{-3})	0.000	0.001
$(\Delta/\sigma)_{max}$		

^{1}H NMR spectra and ^{13}C NMR proton-decoupled spectra were acquired with single-pulse excitation and 30° flip angle. 1 Hz exponential weighting was applied prior to Fourier transformation in carbon spectra. Gradient selected DQF-COSY spectra were acquired with cosygpmfqf pulse program (pulse programs refer to original ones installed by Bruker). Gradient selected NOESY spectra were acquired with noesygpph pulse program. Gradient selected ^{1}H–^{13}C HSQC spectra were acquired with hsqcetgpsisp.2 pulse program (using shaped pulses). Gradient selected ^{1}H–^{13}C HMBC spectra were acquired with hmbcgplpndqf pulse program.

2.5. MS studies

The electron ionization (EI) mass spectra were recorded on a VG ZABSpec mass spectrometer (VG Analytical, Division of Fisons, Manchester, UK), that was equipped with Opus V3.3X program package (Fisons Instruments, Manchester, UK).

2.6. Molecular modeling

Multiple alignment was performed with Muscle[20] and MOE Molecular Operating Environment.[21] Crystal structure of AMPA GluA2 receptor (PDB ID: 3KG2[12]) was selected as the main template. Additional templates were used for N-terminal domain (crystal structure of the GluK2/GluK5 NTD tetramer assembly, PDB ID: 3QLV[22]) and ligand binding domain (crystal structure of GluK1 ligand-binding domain (S1S2) in complex with an antagonist, PDB ID: 4DLD[23]). Homology modeling was carried out with Modeller v. 9.11.[24] Input conformations of the investigated compounds were prepared using the LigPrep protocol from the Schrodinger Suite.[25] To sample different protonation states of ligands in physiological pH Epik module was used.[26] The molecular structures of the investigated compounds in the ground state (in vacuo) were further optimized with the B3LYP DFT (the variant of DFT method using Becke's three parameter hybrid functional (B3)[27] with correlation functional such as the one proposed by Lee, Yang, and Parr (LYP)[28]) using 6-31G(d,p) as included in GAUSSIAN 09.[29] Molecular docking was performed with Glide from the Schrodinger Suite. Ligand-receptor complexes were inserted into POPC lipid bilayer and water with Schrodinger suite of programs and sodium and potassium ions were added to balance protein charges and then till concentration of 0.15 M. The stability of ligand-receptor complexes was assessed by molecular dynamics simulations with Desmond v. 3.0.3.1.[30] The ligands-receptor complexes in lipid bilayer were minimized and subjected to MD first in the NVT ensemble for 1 ns and then in NPT ensemble for 20 ns.

The following software were also used for visualization of results: Chimera v.1.5.3,[31] Mercury v.2.4,[32] VegaZZ v.2.4.0.25,[33] Yasara Structure v.11.9.18,[34] PyMol v.0.99,[35] Discovery Studio v. 3.1[36] and ArgusLab.[37]

3. Results and discussion

3.1. X-ray investigation

For X-ray evaluation we chose 2-methoxyphenyl-3-methyl-5-methoxy-indole derivatives **5** and **6** because they differ considerably in their GluK1/GluK2 kainate receptor affinity. The complete crystal structure analysis of these compounds was expected to yield information concerning the conformation and especially mutual orientation of pharmacophoric aromatic substituents. The X-ray investigation revealed that the compound **5** crystallizes in

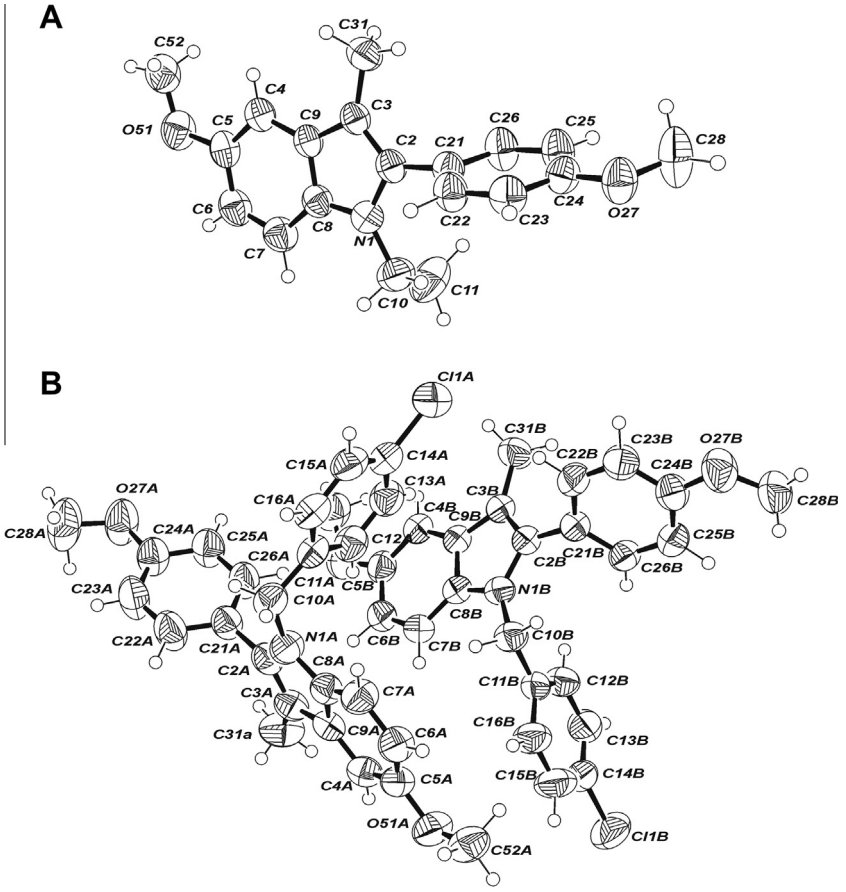

Figure 3. A view of the molecules **5** (A) and **6** (B) with the atomic labelling. Non-H atoms are represented by displacement ellipsoids of 50% probability.

Table 3
Selected torsion angles [°] for **5** and **6** in their crystals

Torsion angles	**5**	**6**A	**6**B
N1–C2–C21–C22	−75.85(18)	90.5(3)	−121.6(2)
C4–C5–O51–C52	−4.6(2)	−179.0(2)	−13.7(3)
C23–C24–O27–C28	−176.5(2)	6.3(5)	−166.8(2)
C2–N1–C10–C11	−90.9(2)	−101.8(2)	−111.2(2)
N1–C10–C11–C12		23.0(3)	22.1(3)

Table 4
Intermolecular interaction geometry (Å, °) for **6**

D–H···A	D-H	H···A	D···A	D-H···A
C22–H221···Cg1	0.99(2)	2.836(19)	3.6592(16)	141.6(17)
C23–H231···Cg2$^{(i)}$	1.00(2)	2.90(3)	3.7637(16)	145.8(19)
C25–H251···Cg$^{(ii)}$	0.96(2)	2.62(3)	3.5078(17)	154(2)
C26–H261···Cg1$^{(ii)}$	0.97(2)	2.79(3)	3.5695(16)	137.7(18)

Symmetry codes: (i) 1−*x*, −1/2 + *y*, 1/2−*z*; (ii) 1−*x*, 1/2 + *y*, 1/2−*z*.
Cg1–centroid of the pyrrole ring; Cg2–centroid of the benzene ring C4···C9.

chiral $P2_12_12_1$ space group, while the compound **6** crystallizes in $P\bar{1}$ space group with two molecules A and B in the asymmetric part of the unit cell. The view of the molecules with numbering of the atoms are shown in Figure 3. The 2-methoxyphenyl-3-methyl-5-methoxy-indole part is common for both analyzed structures and the geometry of this molecular fragment in **5** and **6** is very similar. Its conformation is described by three torsion angles

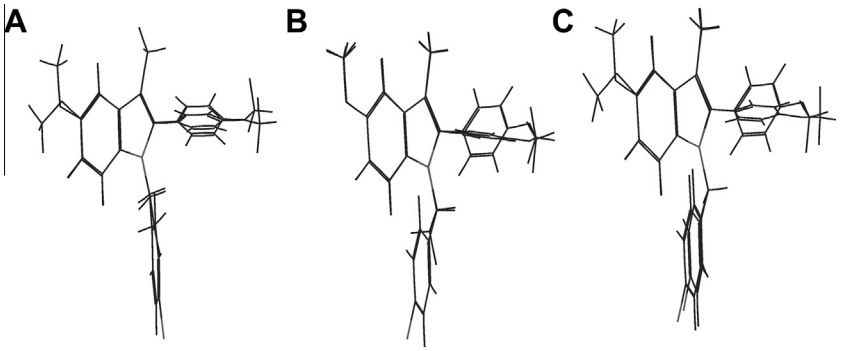

Figure 4. Overlay of molecules **5** and **6A** (A), **5** and **6B** (B) and **6A** and **6B** (C) by least-squares fitting of the indole rings.

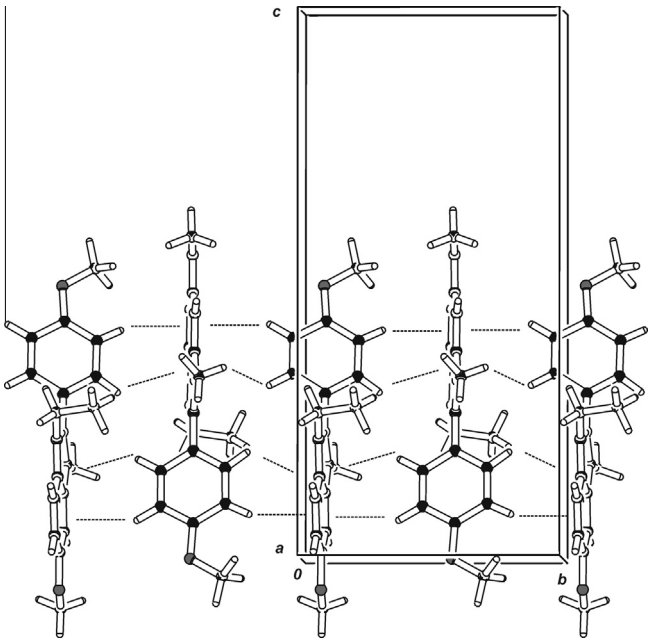

Figure 5. Unit-cell packing in crystal of **5**. Dashed lines indicate C–H···π intermolecular interactions.

Table 5
Hydrogen-bond geometry (Å, °) for **6**

D–H···A	D–H	H···A	D···A	D–H···A
C12A–H12A···N1A	0.93	2.58	2.902(3)	101
C12B–H12B···N1B	0.93	2.58	2.899(3)	101
C25B–H25B···O51A^{i}	0.93	2.49	3.409(3)	168

Symmetry codes: (i) 1−*x*, −*y*, 1−*z*.

N1–C2–C21–C22, C4–C5–O51–C52 and C23–C24–O27–C28 (Table 3). The first one with −75.85(18)° for **5**, 90.5(3)° for **6**A and −121.6(2)° for **6**B indicates similar spatial orientation of the 2-methoxyphenyl substituent in relation to the fused bicyclic system in **5** and **6**B, and slightly different in **6**A. The other two torsion angles show the same, respectively, *cis* and *trans* conformation of the both methoxy groups in **5** and **6**B and opposite *trans* and *cis* conformation of these substituents in **6**A. The similarities and differences in the conformation of the investigated molecules **5** and **6** (A and B) are shown in Figure 4. The chlorobenzyl substituent in **6** adopts *gauche-trans* conformation with respect to the indole ring with torsion angles C2–N1–C10–C11 of −101.8(2), −111.2(2)° and N1–C10–C11–C12 of 23.0(3) and 22.1(3)° for A and B molecules, respectively. This conformation is stabilized by the respective C12–H16···N1 intramolecular hydrogen bonds in molecule A and B (Table 4).

The planar indole ring system is slightly folded along the junction C8–C9; the dihedral angle between the six- and five-membered rings being 1.16(5)° for **5**, 0.83(6)° for **6A** and 1.71(6)° for **6B**. The classic hydrogen bonds are not present in the crystal structure of **5**. Phenyl and indole rings in the crystal of **5** located perpendicularly to each other belonging to the molecules related by 2_1 axis parallel to [010] direction interact via C–H···π interactions (Table 3). Aromatic C22–H221 and C23–H231 from one side and C25–H251 and C26–H261 groups from the other side of the indole ring are involved in these type of interaction (Fig. 5). Similar interactions were found in the crystal structure of **6**. They are accompanied by C–H···O intermolecular hydrogen bonds (Table 5) linking into pairs inversion-related molecules A and B (Fig. 6).

3.2. NMR spectra

All studied compounds were fully characterized by NMR spectroscopy. The assignment of ^{1}H and ^{13}C NMR chemical shifts were done by the aid of techniques DQF-COSY, HSQC, HMBC and NOESY. ^{1}H NMR spectrum consisted of signals from aromatic indole core and different substituents. In a case of 3-methylindole, the proton

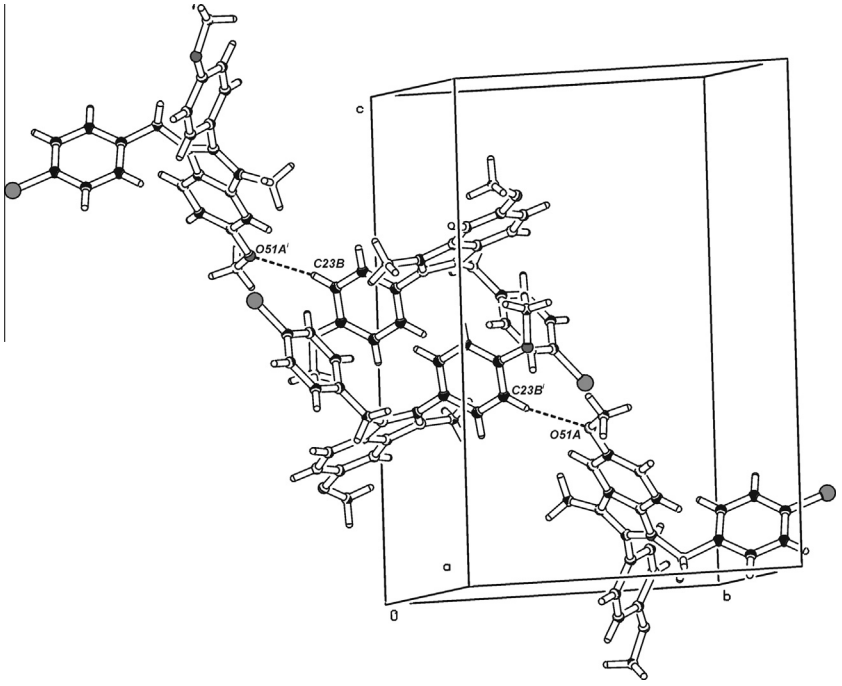

Figure 6. Unit-cell packing in crystal of **6**. Dashed lines indicate C–H···O intermolecular hydrogen bonds.

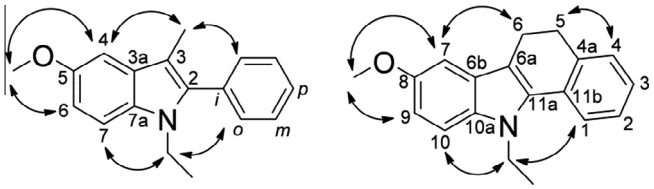

Figure 7. Numbering system and observed NOESY correlations (in arrows) for compounds **9** and **10**.

signals can be easily identified based on coupling constants. When 3-methyl was lacking, DQF-COSY information was needed to assign indole protons. All substituents had their own characteristic proton signals (arom-CH3: 2.1–2.5 ppm; OCH3: 3.8–4.0 ppm; CH2CH3: 1.1–1.4 and 4.0–4.2 ppm; aromatic signals 6.9–7.7 ppm). When the proton signals were assigned, HSQC provided directly corresponding proton bearing carbons. The quaternary carbons were thereafter assigned based on the long range $^{1}H-^{13}C$ correlations from HMBC spectrum. Finally, the assignments were proved by observed NOESY cross peaks. As an example, decisive NOESY correlations are presented for compounds **9** and **10** in Figure 7. This figure shows also the numbering of the structures which is adopted in Tables 6–9.

3.3. MS spectra

All of the compounds **1**–**10** do not show many fragments. In all cases the molecular ion forms the base peak of the spectrum and double-charged molecular ion is always present (4–10%) although for **6** it is very weak. $[M-H]^+$ ion is also abundant when $R^1 = H$ (**2**–**4**) or in the case of compound **10** which also explains why this ion is the most abundant for **4**. Somehow $R^3 = H$ (**1**, **6**) seems to limit the formation of the $[M-H]^+$ ion. In the other compounds this ion is not very abundant since in all of them R^1 is other than H and R^3 equal to methyl. Compound **8** for which $R^3 = CH_3$ and $R^4 = H$ (like for compound **2**) gives 12% of $[M-H]^+$ ion. All compounds also exhibit the ion $[M-CH_3]^+$ which is fairly abundant for compounds **1**–**3** but very weak for four-membered compound **4**. The $[M-CH_3]^+$ ion is missing from the spectrum of compound **6** due to the dominant loss of the $R^1 = CH_2C_6H_4CL$-*p* corresponding to *m*/*z* 266 (54%). The loss of methyl can occur from

Table 6
^{1}H NMR data (chemical shifts, *multiplicity and coupling constants*) for compounds **1**–**3** and **5**–**9** in $CDCl_3$ and at 25 °C (TMS = 0.00 ppm)

Compound	H-3/3-Me	H-4	H-5/5-OMe	H-6	H-7	H-*ortho**	H-*meta**	H-*para**	Others
1	6.76	7.09	3.87	6.86	7.28	7.64	7.43	7.31	[a]
	br. s	*d 2.5*	*s*	*dd 2.5, 8.8*	*d 8.8*	*d 7.5*	*t 7.5*	*t 7.5*	
2	2.43	7.58	7.13	7.19	7.35	7.51	7.01	—	[b]
	s	*d 7.8*	*dd 7.2, 7.8*	*dd 7.2, 8.0*	*d 8.0*	*d 8.8*	*d 8.8*		
3	2.44	7.35	3.90	6.87	7.26	7.57	7.47	7.35	[c]
	s	*d 2.4*	*s*	*dd 2.4, 8.7*	*d 8.7*	*d 7.5*	*t 7.5*	*t 7.5*	
5	2.20	7.03	3.89	6.89	7.24	7.31	7.02	—	[d]
	s	*d 2.4*	*s*	*dd 2.4, 8.8*	*d 8.8*	*d 8.7*	*d 8.7*		
6	2.26	7.05	3.89	6.81	7.02	7.21	6.93	—	[e]
	s	*d 2.4*	*s*	*dd 2.4, 8.8*	*d 8.8*	*d 8.7*	*d 8.7*		
7	6.45	7.11	3.87	6.90	7.29	7.49	7.46	7.40	[f]
	br. s	*d 2.4*	*s*	*dd 2.4, 8.8*	*d 8.8*	*d 7.4*	*t 7.4*	*t 7.4*	
8	2.23	7.59	7.14	7.23	7.35	7.32	7.02	—	[g]
	s	*d 7.8*	*dd 7.2, 7.8*	*dd 7.2, 8.0*	*d 8.0*	*d 8.8*	*d 8.8*		
9	2.21	7.04	3.89	6.90	7.25	7.39	7.48	7.41	[h]
	s	*d 2.4*	*s*	*dd 2.4, 8.8*	*d 8.8*	*d 7.6*	*t 7.6*	*t 7.6*	

* Only vicinal couplings are presented for substituted aryl group protons.
[a] 8.22 (br s, NH).
[b] 3.87 (s *p*-OMe), 7.94 (br s, NH).
[c] 7.90 (br s, NH).
[d] 1.19 (t 7.2, CH_3), 3.88 (s *p*-OMe), 4.02 (q 7.2, CH_2).
[e] 3.84 (s *p*-OMe), 5.14 (s CH_2), 6.85 (d 8.5, H-2′), 7.18 (d 8.5, H-3′).
[f] 1.31 (t 7.2, CH_3), 4.17 (q 7.2, CH_2).
[g] 1.21 (t 7.2, CH_3), 3.89 (s *p*-OMe), 4.06 (q 7.2, CH_2).
[h] 1.18 (t 7.1, CH_3), 4.03 (q 7.1, CH_2).

Table 7
^{13}C NMR chemical shifts for compounds **1**–**3** and **5**–**9** in $CDCl_3$ and at 25 °C (TMS = 0.00 ppm)

Compound	C-2	C-3	C-3a	C-4	C-5	C-6	C-7	C-7a	C-3-Me	C-5-OMe	C-ipso	C-*ortho*	C-*meta*	C-*para*	Others
1	138.61	99.85	129.73	102.25	154.51	112.64	111.63	132.00	—	55.84	132.44	125.06	129.02	127.65	—
2	133.99	107.75	130.06	118.74	119.44	121.96	110.50	135.64	9.59	—	125.91	129.00	114.28	158.98	[a]
3	134.97	108.50	130.42	100.83	154.14	112.44	111.44	131.00	9.76	55.97	133.40	127.66	128.80	127.28	—
5	137.76	108.11	128.81	100.80	153.87	111.42	110.16	130.89	9.32	56.08	124.76	131.64	113.82	159.24	[b]
6	138.24	108.70	129.20	100.85	154.15	111.75	110.66	131.78	9.49	55.96	124.11	131.59	113.88	159.35	[c]
7	141.67	101.73	128.60	102.27	154.27	111.79	110.62	132.44	—	55.94	133.22	129.27	128.49	127.88	[d]
8	136.96	108.47	128.65	118.76	118.92	121.35	109.37	135.79	9.24	—	124.67	131.71	113.82	159.25	[e]
9	137.92	108.41	128.35	100.86	153.91	111.67	110.27	131.33	9.32	56.05	132.53	130.47	128.35	127.76	[f]

[a] 55.37 (*p*-OMe).
[b] 15.45 (CH_3), 38.65 (CH_2), 55.31 (*p*-OMe).
[c] 46.99 (CH_2), 55.29 (*p*-OMe), 127.39 (C-2′), 128.72 (C-3′), 132.71 (C-4′), 137.19 (C-1′).
[d] 15.47 (CH_3), 38.88 (CH_2).
[e] 55.31 (*p*-OMe).
[f] 15.42 (CH_3), 38.74 (CH_2).

Table 8
^{1}H NMR data (chemical shifts, *multiplicity and coupling constants*) for compounds **4** and **10** in $CDCl_3$ and at 25 °C (TMS = 0.00 ppm)

Compound	H-1	H-2	H-3 / 3-OMe	H-4	H-5	H-6	H-7	H-8-OMe	H-9	H-10	Others
4	7.28	7.23	7.15	7.26	3.05	2.94	6.99	3.87	6.84	7.24	[a]
	dd 1.4, 7.6	*t 7.6*	*dt 1.4, 7.6*	*d 7.6*	*br t 7.2*	*m*	*d 2.4*	*s*	*dd 2.4, 8.8*	*d 8.8*	
10	7.52	7.30	7.17	7.32	2.96	2.87	7.01	3.88	6.88	7.26	[b]
	dd 1.2, 7.8	*dd 7.4, 7.8*	*dt 1.4, 7.4*	*d 7.4*	*m*	*m*	*d 2.4*	*s*	*dd 2.4, 8.8*	*d 8.8*	

[a] 8.07 (br s NH).
[b] 1.51 (t 7.1, CH_3), 4.41 (q 7.1, CH_2).

Table 9
^{13}C NMR chemical shifts for compounds **4** and **10** in $CDCl_3$ and at 25 °C (TMS = 0.00 ppm)

Compound	C-1	C-2	C-3	C-4	C-4a	C-5	C-6	C-6a	C-6b	C-7	C-8	C-9	C-10	C-10a	C-11a	C-11b	Others
4	119.75	126.66	126.62	128.47	136.47	29.55	19.72	112.48	128.94	100.59	154.30	112.40	111.82	132.11	133.87	127.77	[a]
10	121.97	126.73	126.18	128.71	138.18	30.78	20.17	113.66	126.37	100.43	154.12	112.25	110.28	133.70	134.74	129.66	[b]

[a] 55.89 (8-OMe).
[b] 15.74 (CH_3), 39.83 (CH_2), 55.93 (8-OMe).

Table 10
Electron impact mass spectra of 4 2,3,5-trisubstituted **1**–**4** and 6 1,2,3,5-tetrasubstituted indoles **5**–**10**

Compound	$M^{+\cdot}$	M^{2+}	$[M-H]^+$	$[M-CH_3]^+$	$[M-C_2H_3O]^+$	$[M-R^1-C_2H_3O]^+$	$[M-R^3-CH_3O]^{+\cdot}$	$[M-H-R^1-C_2H_3O]^+$	$[M-R^2]^+$	$[M-H-R^1]^+$
1	223(100)	111.6(8)	222(4)	208(24)	180(47)	179(5)	191(6)	–	–	–
2	237(100)	118.5(7)	236(34)	222(25)	194(5)	193(9)	191(7)	192(7)	130(5)	–
3	237(100)	118.6(8)	236(22)	222(27)	–	193(9)	191(7)	–	160(5)	–
4	249(100)	124.3(10)	248(61)	234(4)	206(12)	205(13)	217(9)[a]	204(14)	–	247(6)[d]
5	295(100)	147.5(9)	294(6)	280(22)	252(8)	–	249(5)	–	–	–
6	391(100)	Very weak	390(2)	–	–	223(9)	–	–	–	–
7	251(100)	125.7(8)	250(2)	236(42)	208(14)	179(6)	193(6)[b]	204(14)	–	–
8	265(100)	132.6(4)	164(12)	250(28)	–	193(4)	219(8)[b]	192(5)	–	235(8)
9	265(100)	132.5(6)	264(7)	250(34)	222(9)	193(6)	–	192(5)	–	–
10	277(100)	138.7(8)	276(28)	262(18)	234(6)	205(8)	217(5)[c]	204(11)	248(6)	247(5)

Other fragments for **1**: $[M-H-R^1-C_4H_5O]^+$ 152(8), Ph^+(6); **2**: $[M-H-C_4H_5O]^+$ 167(7); **4**: $[M-H-CH_3]^{+\cdot}$ 233(6), $[M-C_2H_3O-C_8H_8]^{+\cdot}$ 152(8); **6**: 267(11), $[M-R^1]^+$ 266(54), $[M-R^1-R^3]^{+\cdot}$ 251(6), $[M-H-R^1-R^4-C_2H_3O]^{+\cdot}$ 191(6), $[R^1]^+$ 125(17); **7**: $[M-CH_3-C_2H_3O]^{+\cdot}$ 193(6), $[M-H_2-C_4H_5O]^{+\cdot}$ 180(5); **8**: $[M-H-CH_3-R^1]^+$ 220(6), $[M-H-R^1-CH_3O]^{+\cdot}$ 204(6), $[M-H_2-R^1-C_2H_3O]^+$ 191(7). $[M-H_2-C_4H_5O]^{+\cdot}$ 180(5); **10**: $[M-H_2]^{+\cdot}$ 275(6), $[M-R^1]^+$ 248(6), $[M-R^1-CH_3O]^{+\cdot}$217(5).
[a] $[M-R^1-CH_3O]^{+\cdot}$.
[b] $[-CH_3-CH_3O]^{+\cdot}$.
[c] $[M-C_2H_5-CH_3O]^{+\cdot}$.
[d] $[M-H_2]^{+\cdot}$.

the methoxy groups (**1**, **7**, **8**, **9** and **10**) and to some extent also from the loss of R^3 (**2**, **3**, **5**, **8** and **9**) or from $R^1 = C_2H_5$ (**5**, **7**, **8**, **9** and **10**). Compounds **1**, **2**, **4**, **5**, **7**, **9** and **10** exhibit the ion $[M-C_2H_3O]^+$ which is strongest for **2** (47%) and all compounds except **5** give also relatively weak ion $[M-R^1-C_2H_3O]^{+\cdot}$. Compounds **1**–**5** and **8** exhibit also some amounts of the ion $[M-R^3-CH_3O]^{+\cdot}$. It is interesting that only **2** and **3** show small amount of the ion $[M-R^2]^+$ (Table 10). Compounds **2**, **4**, **8**–**10** exhibit also the ion $[M-H-R^1-C_2H_3O]^+$. It is interesting that both four-membered derivatives **4** and **10** exhibit the ion $[M-H_2]^{+\cdot}$ which proves that the origin of this ion must be other than $[M-H-R^1]^{+\cdot}$ as it is for **8** and **10**. A few more ions can be observed for most of the compounds as shown below Table 10.

3.3.1. Homology modeling

Homology models of GluK1 and GluK2 receptors were built on novel AMPA GluA2 receptor template with application of additional kainate receptor templates for ligand binding domain and N-terminal domain (see Experimental section for details). Sequences identity between the GluA2 template and GluK1 and GluK2 receptors was 39.73% and 40.58% respectively. To our knowledge, these are first kainate receptor models built on novel AMPA receptor template.

Homology models of GluK1 and GluK2 receptors have similar architecture to the used GluA2 receptor template and differ significantly from previously constructed models based on separate templates for each domain.[10,11] However, they are also characterized by dimer of dimers topology. They consist of N-terminal domain, ligand-binding domain, transduction domain and transmembrane domain. The final model of GluK2 receptor, a very similar to GluK1 receptor model, is presented in Figure 8.

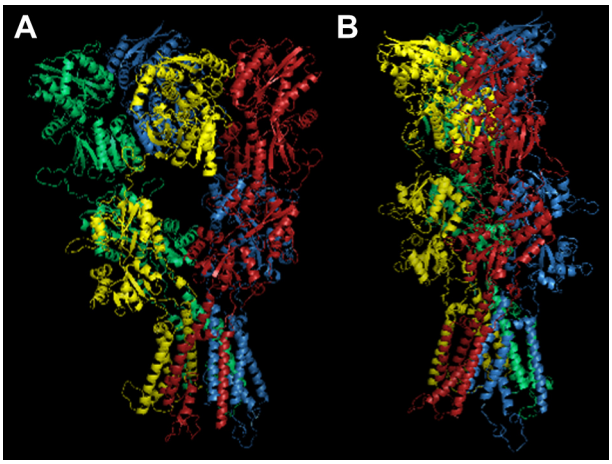

Figure 8. Homology model of GluK2 receptor, A-front view; B-side view.

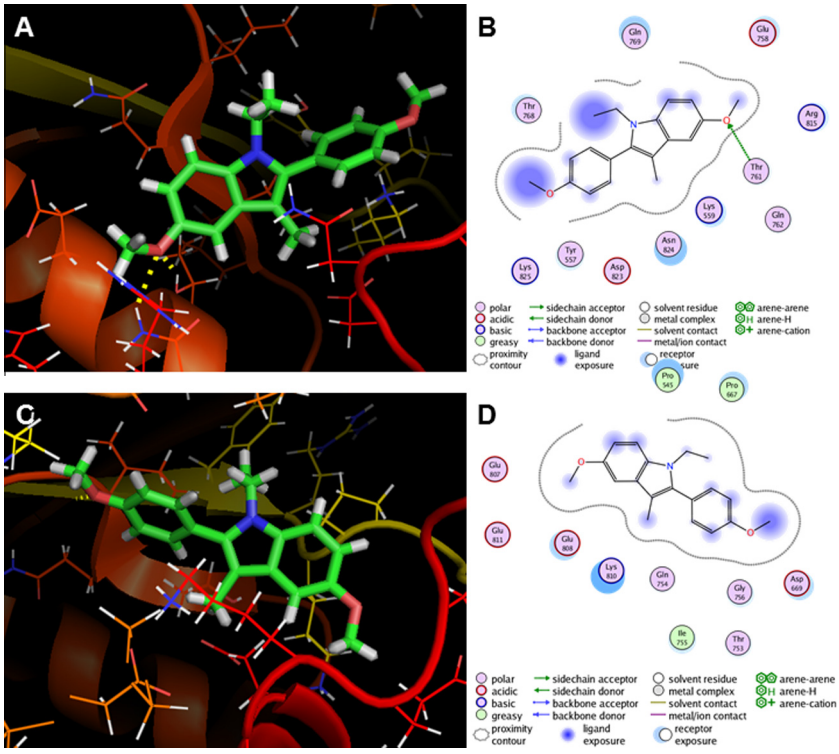

Figure 9. Compound **5** in the binding pocket of GluK1 (A, B) and GluK2 (C, D) receptor.

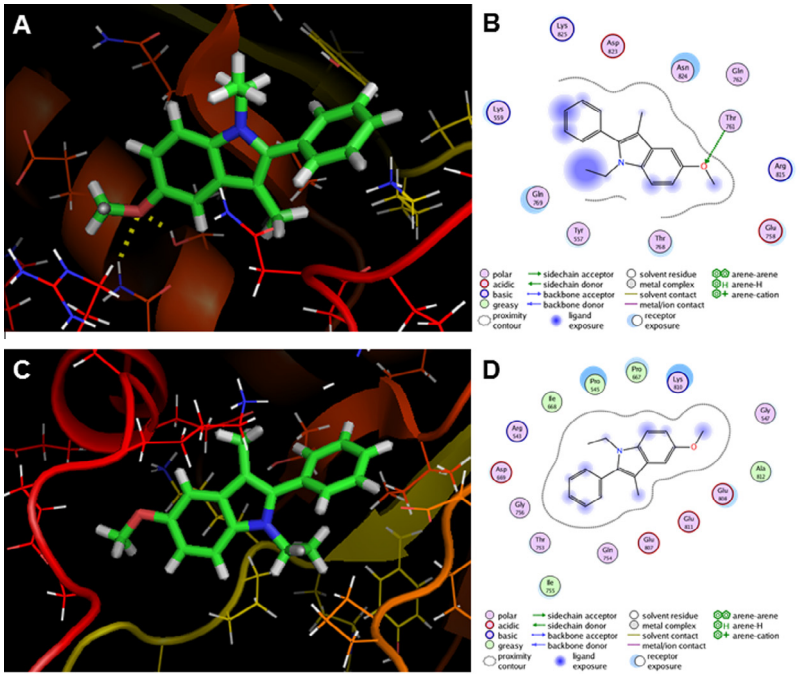

Figure 10. Compound **7** in the binding pocket of GluK1 (A, B) and GluK2 (C, D) receptor.

3.3.2. Ligand-receptor interactions

The binding site for non-competitive GluK1/GluK2 receptors was identified in the receptor transduction domain, that is, in the domain which connects ligand-binding domain and transmembrane domain. This assumption was made on the basis of studies by Balannik et al.[38] for AMPA receptors as well as on our earlier molecular modelling studies.[10] The exact binding site was found on the basis of sequence differences between GluK1 and GluK2 receptors in the transduction domain. There are no differences in S1-M1 linker and in S2-M4 linker Asp823 and Asn824 in GluK1 corresponds to Glu808 and Ser809 in GluK2. Indeed, these residues were found in the binding pocket (Figs. 9 and 10). In case of GluK1 receptor it was determined that the pharmacophoric[9] methoxy group at position 5 interacts via the hydrogen bond with the side

chain of Thr761. This was true for all the compounds having methoxy group at this position and it is in contrast with earlier studies. In case of GluK2 receptor an analogous interaction was not identified but some residues turned out to have potential for such contacts (like the main chain nitrogen atom of Ala812). Instead, the derivatives having methoxy group at position 2 formed hydrogen bond with the main of Glu756. Further derivatives which complete the binding pockets for both receptors can be found in Figures 9 and 10 drawn for derivatives **5** and **7**. It was also determined that inactive derivatives **6** (with chlorobenzyl derivative in position 1) and **10** (carbazol derivatives) are too big to adopt well to the binding pocket. In contrast to our previous molecular docking studies,[11] it was found that the binding pocket for non-competitive antagonists is situated within one receptor subunit, not on the border of two subunits. The stability of ligand-receptor complexes was confirmed in short molecular dynamics simulations.

4. Conclusions

In this Letter we performed extensive structural studies of novel indole-derived non-competitive antagonist of GluK1 and GluK2 receptors in view of their pharmacological activity. We also built the first homology model of kainate receptors based on the novel AMPA receptor template. Furthermore, we identified the site of allosteric modification of kainate receptors in the transduction domain. The obtained results are of crucial relevance for elaboration of more potent non-competitive antagonists of GluK1 and GluK2 receptors as the constructed models may be used in future structure-based drug design studies. The presented compounds may find application as pharmacological tools to study kainate receptors and as lead compounds for further modifications.

Acknowledgments

This work was funded by the Polish Ministry of Science and Higher Education, grant number 405 021 31/1121. The paper was developed using the equipment purchased within the project 'The equipment of innovative laboratories doing research on new medicines used in the therapy of civilization and neoplastic diseases' within the Operational Program Development of Eastern Poland 2007–2013, Priority Axis I Modern Economy, operations I.3 Innovation promotion. The research was partially prepared during the postdoctoral fellowship of Agnieszka A. Kaczor at University of Eastern Finland, Kuopio, Finland under Marie Curie fellowship. Calculations were partially performed under a computational grant by Interdisciplinary Center for Mathematical and Computational Modeling (ICM), Warsaw, Poland, grant number G30-18. Desmond calculations were performed using resources of CSC, Finland.

References and notes

1. Kaczor, A. A.; Matosiuk, D. *Curr. Med. Chem.* **2010**, *17*, 2608.
2. Kew, J. N. C.; Kemp, J. A. *Psychopharmacology (Berl.)* **2005**, *179*, 4.
3. Stawski, P.; Janovjak, H.; Trauner, D. *Bioorg. Med. Chem.* **2010**, *18*, 7759.
4. Jane, D. E.; Lodge, D.; Collingridge, G. L. *Neuropharmacology* **2009**, *56*, 90.
5. Matute, C. *CNS Neurosci. Ther.* **2011**, *17*, 661.
6. Szénási, G.; Vegh, M.; Szabo, G.; Kertesz, S.; Kapus, G.; Albert, M.; Greff, Z.; Ling, I.; Barkoczy, J.; Simig, G.; Spedding, M.; Harsing, L. G., Jr. *Neurochem. Int.* **2008**, *52*, 166.
7. Valgeirsson, J.; Nielsen, E. Ø.; Peters, D.; Varming, T.; Mathiesen, C.; Kristensen, A. S.; Madsen, U. *J. Med. Chem.* **2003**, *46*, 5834.
8. Valgeirsson, J.; Nielsen, E. O.; Peters, D.; Mathiesen, C.; Kristensen, A. S.; Madsen, U. *J. Med. Chem.* **2004**, *47*, 6948.
9. Kaczor, A. A.; Kronbach, C.; Unverferth, K.; Pihlaja, K.; Wiinamaki, K.; Sinkkonen, J.; Kijkowska-Murak, U.; Wróbel, T.; Stachal, T.; Matosiuk, D. *Lett. Drug Des. Discov.* **2012**, *9*, 891.
10. Kaczor, A. A.; Kijkowska-Murak, U. A.; Kronbach, C.; Unverferth, K.; Matosiuk, D. *J. Chem. Inf. Model.* **2009**, *49*, 1094.
11. Kaczor, A. A.; Kijkowska-Murak, U. A.; Matosiuk, D. *J. Med. Chem.* **2008**, *51*, 3765.
12. Sobolevsky, A. I.; Rosconi, M. P.; Gouaux, E. *Nature* **2009**, *462*, 745.
13. Sheldrick, G.M. SADABS, Ver. 2.06. University of Göttingen, Germany 2002.
14. Altomare, A.; Cascarano, G.; Giacovazzo, C.; Guagliardi, A. J. *Appl. Cryst.* **1993**, *26*, 343.
15. Sheldrick, G. M. *Acta Cryst.* **2007**, *64*, 112.
16. Flack, H. D. *Acta Cryst.* **1983**, *39*, 876.
17. Farrugia, L. J. J. *Appl. Cryst.* **1997**, *30*, 565.
18. Nardelli, M. *Comp. Chem.* **1983**, *7*, 95.
19. Spek, A. L. J. *Appl. Cryst.* **2003**, *36*, 7.
20. Edgar, R. C. *Nucleic Acids Res.* **2004**, *32*, 1792.
21. MOE Molecular Operating Environment 2009.10, Chemical Computing Group.
22. Kumar, J.; Schuck, P.; Mayer, M. L. *Neuron* **2011**, *71*, 319.
23. Venskutonytė, R.; Frydenvang, K.; Valadés, E. A.; Szymańska, E.; Johansen, T. N.; Kastrup, J. S.; Pickering, D. S. *ChemMedChem* **2012**, *7*, 1793.
24. Eswar, N.; Marti-Renom, M. A.; Webb, B.; Madhusudhan, M. S.; Eramian, D.; Shen, M.; Pieper, U.; Sali, A. *Current Protocols in Bioinformatics* Suppl 15; John Wiley & Sons Inc, 2006; pp 5.6.1–5.6.30.
25. LigPrep, Version 2.4: Schrödinger, LLC, New York, **2010**.
26. Epik, Version 2.1: Schrödinger, LLC, New York, **2010**.
27. Becke, A. *J. Chem. Phys.* **1993**, *98*, 5648.
28. Lee, C.; Yang, W.; Parr, R. G. *Phys. Rev. B Condens. Matter* **1988**, *37*, 785.
29. GAUSSIAN 09, Revision A.1 Frisch, M. J.; Trucks, G. W.; Schlegel, H. B.; Scuseria, G. E.; Robb, M. A.; Cheeseman, J. R.; Scalmani, G.; Barone, V.; Mennucci, B.; Petersson, G. A.; Nakatsuji, H.; Caricato, M.; Li, X.; Hratchian, H. P.; Izmaylov, A. F.; Bloino, J.; Zheng, G.; Sonnenberg, J. L.; Hada, M.; Ehara, M.; Toyota, K.; Fukuda, R.; Hasegawa, J.; Ishida, M.; Nakajima, T.; Honda, Y.; Kitao, O.; Nakai, H.; Vreven, T.; Montgomery, J. A., Jr.; Peralta, J. E.; Ogliaro, F.; Bearpark, M.; Heyd, J. J.; Brothers, E.; Kudin, K. N.; Staroverov, V. N.; Kobayashi, R.; Normand, J.; Raghavachari, K.; Rendell, A.; Burant, J. C.; Iyengar, S. S.; Tomasi, J.; Cossi, M.; Rega, N.; Millam, J. M.; Klene, M.; Knox, J. E.; Cross, J. B.; Bakken, V.; Adamo, C.; Jaramillo, J.; Gomperts, R.; Stratmann, R. E.; Yazyev, O.; Austin, A. J.; Cammi, R.; Pomelli, C.; Ochterski, J. W.; Martin, R. L.; Morokuma, K.; Zakrzewski, V. G.; Voth, G. A.; Salvador, P.; Dannenberg, J. J.; Dapprich, S.; Daniels, A. D.; Farkas, Ö.; Foresman, J. B.; Ortiz, J. V.; Cioslowski, J.; Fox, D. J; Gaussian Inc: Wallingford CT, 2009.
30. Bowers, K. J.; Chow, E.; Xu, H.; Dror, R. O.; Eastwood, M. P.; Gregersen, B. A.; Klepeis, J. I.; Kolossváry, I.; Moraes, M. A.; Sacerdoti, F. A.; Salmon, J. K.; Shan, Y.; Shaw, D. E. Scalable Algorithms for Molecular Dynamics Simulations on Commodity Clusters, Proceedings of the ACM/IEEE Conference on Supercomputing (SC06), Tampa, Florida, November 11–17, 2006.
31. Pettersen, E. F.; Goddard, T. D.; Huang, C. C.; Couch, G. S.; Greenblatt, D. M.; Meng, E. C.; Ferrin, T. E. *J. Comput. Chem.* **2004**, *25*, 1605.
32. Macrae, C. F.; Bruno, I. J.; Chisholm, J. A.; Edgington, P. R.; McCabe, P.; Pidcock, E.; Rodriguez-Monge, L.; Taylor, R.; Van De Streek, J.; Wood, P. A. J. *Appl. Cryst.* **2008**, *41*, 466.
33. Pedretti, A.; Villa, L.; Vistoli, G. *J. Comput. Aided Mol. Des.* **2004**, *18*, 167.
34. Krieger, E.; Vriend, G. *Bioinformatics* **2002**, *18*, 315.
35. The PyMOL Molecular Graphics System, Version 0.99, Schrödinger LLC.
36. Discovery Studio 3.1, Accelrys.
37. http://www.arguslab.com/arguslab.com/ArgusLab.html.
38. Balannik, V.; Menniti, F. S.; Paternain, A. V.; Lerma, J.; Stern-Bach, Y. *Neuron* **2005**, *48*, 279.